

Irregular scattering of electrons on ions in a laser field and enhanced inverse Bremsstrahlung heating rates

A. B. Brantov, W. Rozmus, R. Sydora, and C. E. Capjack
 Theoretical Physics Institute, Department of Physics,
 University of Alberta, Edmonton, T6G 2J1, Alberta, Canada
 V. Yu. Bychenkov
 P. N. Lebedev Physics Institute, Russian Academy of Science,
 Moscow 117924, Russia
 V. T. Tikhonchuk
 Institut de Physique Fondamentale, Université Bordeaux I, France
 (December 14, 2018)

Test particle calculations have been performed of classical electron trajectories in the combined field of an ion and a homogeneous, high frequency laser field. By taking ensemble averages with respect to initial conditions, inverse bremsstrahlung heating rates are found and are compared with several known analytical and numerical results. The role of stochastic electron trajectories at high laser intensities which involve multiple collisions and large angle scattering events is examined in the calculations of the heating rates. These are important for anisotropic electron distribution functions, such as those produced by photoionization and are statistically negligible in the case of plasmas described by isotropic electron distribution functions. The critical role played by short range cut-offs in determining electron scattering cross sections is also addressed.

I. INTRODUCTION

The description of electron-ion (e-i) collisions in presence of a strong oscillatory electric field has been an essential part of every laser plasma interaction model. Collisional absorption, inverse Bremsstrahlung (IB) heating and transport processes rely on a correct expression for the e-i collision frequency. Advances in laser technology, particularly those related to the generation of ultra short laser pulses and progress in inertial confinement fusion studies have challenged our understanding of collisional processes over a wide range of conditions and plasma parameters. Recently, Framan et al. have published a series of papers [1] identifying a population of electrons in phase space that experience multiple interactions with ions resulting in large angle scattering and anomalously high heating rates. However the role of these correlated collisions in overall heating rate which depends on the electron distribution function has yet to be quantified. In this paper we summarize the known results for energy exchange due to IB and compare these with numerical test particle calculations. We also examine the statistical importance of stochastic electron orbits on the average heating rates and on the kinetic modeling of laser produced plasmas.

Plasma evolution in the presence of high frequency electric fields has been investigated for about forty years starting with pioneering works by Dawson and O'Brien [2] and Silin [3]. In addition to kinetic theories, analytical descriptions of IB heating published during this time period can be roughly divided into two groups: "first principle" quantum mechanical calculations [4,5] and classical mechanics approximations, cf. e.g. [4,6,7]. All theories consider the two body scattering problem as a starting point. Essentially they all calculate the IB heating rate involving only small angle scatterings and weak momentum transfer. Only recently, numerical studies of electron scattering on ions in presence of a high-frequency field [1,8] have revealed a new physics of stochastic electron trajectories and correlated collisions, which may result in large momentum exchange. The statistical weight of these correlated collisions on the average heating rates remains undetermined.

The Dawson-O'Brien (DO) model [2,9,11] of the electron-ion correlation function is based on the classical Born approximation of binary collisions and on an explicit average over random ion positions. The Coulomb field of immobile ions is considered as a weak perturbation to the electron motion with drift velocity v_0 along a straight trajectory together with an oscillation in the laser field with a quiver velocity v_E . The DO collision operator describes e-i scattering as an instantaneous event resulting in a small angle deflection of the electron trajectory. The IB heating rate has been found in the weak field limit [2] or for an arbitrary strength of the oscillating field [10] with a Maxwellian distributions of electrons [2,10] or with arbitrary distribution functions [9,11]. Derivations by Pert [9] and Shvets and Fish [11] arrive at DO-like expressions starting from the test particle, two body scattering problem. A useful review of high field effects on the IB heating rates has been published by Vick et al. [12].

Silin [3] has developed a kinetic model of IB heating independent from the DO work. He has calculated the high frequency nonlinear conductivity and the effective collisional frequency for a fully ionized plasma which is in close agreement with the DO model [10] in both limits of weak and strong high frequency fields.

Several classical descriptions of the effective collisional frequency have been derived from the dynamics of Rutherford electron scattering assuming instantaneous and elastic interactions [4,6,7]. They are identified as the classical approximation [4], the impact approximation [6], or more recently, the ballistic model [7]. From the energy conservation for such collisions one finds that the change in the average electron kinetic energy, which is related to electron drift velocity, is proportional to the change in the electron momentum. Therefore the heating rate can be calculated in terms of the transport cross section. Finding an expression for the IB heating rate also involves an average with respect to the phase of the laser field at the time of the e-i collision. A similar result for the IB heating rate can be obtained from the solution to the electron kinetic equation with a Landau collision operator after averaging the result with respect to the high frequency oscillations [13].

The Rutherford cross section in the classical Coulomb field scattering problem leads to a logarithmic divergence, accounted for by the so-called Coulomb logarithm in the collision frequency. At large distances, the cut-off length appears naturally in kinetic theory due to plasma screening effects as shown in the Balescu-Guemsey-Lenard theory of particle collisions [14]. Similarly, a large amplitude high frequency field introduces another cut-off in the collision operator at large impact parameters [2,3]. However, there is no such limitation at short distances within the framework of classical mechanics. This has to be introduced explicitly by using quantum mechanical or statistical arguments. This is a particularly important point in the classical description because the correlated large angle collisions become important for small impact parameters, as discovered in recent studies [1,8].

Implicit in all previous treatments of e-i collisions in presence of a high frequency field is so-called "low frequency" approximation which considers particle collision as an instantaneous event. Quantum descriptions of e-i collisions in a laser field employing the low frequency approximation have been developed by Kroll and Watson (KW) [5] and by Bunkin and Fedorov who applied the Born approximation with respect to the Coulomb field [4]. Agreement between the quantum mechanical and the classical derivations of the electron heating rate has been demonstrated by Ferrante et al. [16]. They found that the quasi-classical, or eikonal approximation leads in a straightforward manner to the KW formula. This agreement between quantum mechanical calculations and classical orbit integrations will be further demonstrated in our numerical studies.

It is important to recognize that this similarity between quantum and classical mechanical approaches includes an appropriate cut-off value for classical interactions at short distances. For example, the KW expression in the limit of a weak oscillatory field contains a Coulomb logarithm with the de Broglie wavelength as the short distance limit. This approximation applies to fast electrons with energies higher than the atomic binding energy. Such a cut-off must be introduced into the classical calculations of the IB heating rate as an additional condition. For electrons with smaller energies (comparable with the atomic binding energy), free-bound transitions must be taken into account. This further complicates the physics of e-i collisions [15].

Analytical IB heating rates have been averaged with respect to the Maxwellian velocity distribution function [17] showing good agreement between classical and quantum results. However no expressions are available for the scattering cross section of single electron in a laser field and for the IB heating rate for an arbitrary electron distributions.

The common feature of theories cited above is that they all involve assumptions of a small scattering angle, instantaneous collisions and they ignore events with small impact parameters. They fail to describe correlation effects, complicated electron trajectories and large angle scattering. These effects have been studied numerically [1,8] and it was found that they can dominate heating rates for electrons with small drift velocities $v_0 \ll v_E$ that are launched in parallel with the electric field direction. However the statistical weight of these so-called "representative" electrons [1], depends on the electron distribution function. Our analysis shows that the correlation processes might become important for the averaged IB heating of electrons with a strongly anisotropic velocity distribution, such as that produced in photoionized plasma [18]. In contrast, they are not statistically important in isotropic plasmas.

In Section II we discuss various analytical expressions for the IB heating rate and describe our numerical model. Section III is devoted to calculations of energy exchange rates between the laser field and monoenergetic electron beams. Heating rates for strongly anisotropic and isotropic electron distribution functions are also derived. The conclusions are presented in Sec. IV.

II. DESCRIPTION OF THE ENERGY EXCHANGE IN THE LASER FIELD

In the introduction, we identified three groups of analytical results describing e-i collisions in the presence of a homogeneous oscillating electric field. The first group involves "first principle" quantum mechanical calculations [4,5]. The second group includes the seminal work by Dawson and Oberman [2] and papers which develop a kinetic description of the plasma based on approximations to the two body correlation function [10,11]. Finally, works from the third group modify the classical mechanical Rutherford scattering problem to allow for electron oscillations in the laser field [4,6,7]. All these studies are restricted to small angle collisions which involve small momentum exchange.

The three categories are rather broad and are not necessarily clearly separable. For example, we have included in the second category of kinetic studies the Ref. [11] which starts with a test particle formulation and after averaging leads to heating rates similar to those of Refs. [2,10]. Our three groups include all known to us analytical results for e-i collision rates and prove to be a convenient characterization for various formalisms that are used to calculate the heating rate for electrons of a given initial energy. In fact, as we will see below, all theories lead to remarkably similar heating rates particularly for energetic electrons and small angle collisions, where electron scattering is well described by the Born approximation. Distinct from the analytical studies are numerical calculations of particle trajectories and cross sections, in particular, the recent publications by Fraiman et al. [1].

A. Energy absorption rate { quantum and classical treatments

In this section we summarize analytical expressions for the rate of energy exchange between a single electron and a linearly polarized laser field $E = E_0 \cos(\omega t)$ due to e-i scattering in the nonrelativistic approximation.

Quantum mechanical calculations [4,17] describe the energy exchange rate between an electron and a laser field by using the Kramers-Heisenberg cross sections [5] for e-i scattering. The result is given by

$$\frac{d}{dt} = \frac{n_i Z^2 e^4}{2m v_0} \sum_{l=-l_{max}}^{l_{max}} X^{1-Z} \ln \left(\frac{1 + |l|^{j=2}}{1 + |l-2|^{j=2} (1 + |l|^2 n)} \right) J_1^2 \frac{2v_E}{v_0} [(1 + |l|)^{j=2} n^0 - n] ; \quad (1)$$

where n and n^0 refer to the propagation directions of the electron before and after collision, respectively, $\omega = 2\hbar \omega = m v_0^2$, e , m and v_0 are the electron charge, mass and the initial drift velocity, and $l_{max} = 1 + \omega$ is the maximum number of emitted photons. Energy exchange in this equation is expressed in terms of the differences between the total absorption cross section (the term with $l > 0$ in the sum) and emission (the term with $l < 0$) of l photons.

The Dawson-Oberman approach is based on the classical Born approximation for the description of e-i collisions and only takes into account small angle scattering. The IB heating rate for a given electron has the following form [9,11]

$$\frac{d}{dt} = \frac{2n_i Z^2 e^4}{m v_0} \int_0^{\omega} dk J_1^2 \frac{k v_E}{k^2} \frac{n}{\omega} \frac{\partial}{\partial k} \left(\frac{v_0}{\omega} k - n \right) ; \quad (2)$$

where the integration over the transferred momentum k involves the upper cut-off limit at $k_{max} = m v_0^2 = 2Z e^2$, which corresponds to small angle collisions. The general expressions (1) and (2) are rather complicated for detailed investigations and we consider simplified expressions that result for the special cases described below.

Classical theory results from studies by Pert [6] and Bunkin [4] are based on the instantaneous collision approximation and are averaged with respect to the laser field period. The heating rate is given by the following expression:

$$\frac{d}{dt} = \frac{n_i Z^2 e^4}{m} \int_0^{\omega} d \frac{v_E}{(v_0^2 + 2v_E} \frac{n_0 v \cos + v_E^2 \cos^2}{n_0 v \cos + v_E^2 \cos^2)^{3=2}} ; \quad (3)$$

where \ln is the Coulomb logarithm which is calculated in terms of a full electron velocity [7,19]

$$\ln = \ln \left(1 + \frac{b_{max}^2}{b_{min}^2} \right) = \ln \left(1 + m^2 v^6 = 4Z^2 e^4 \omega^2 \right) ; \quad (4)$$

The velocity $v = v_0 n + v_E \cos$ and $b_{max} = v \omega$ and $b_{min} = 2Z e^2 = m v^2$ are the classical cut-offs at large and small impact parameters. For the cut-off at the small distances we use the electron de Broglie wavelength, $b_{min} = \lambda_B = \hbar / m v$ in order to compare our studies with the quantum theory, i. e. instead of the Coulomb logarithm (4) we use $\ln(1 + m^2 v^4 = \hbar^2 \omega^2)$. Equation (3) shows that when the quiver velocity, v_E , reaches the drift velocity, v_0 , the singularity first appears for electrons launched in the direction of the electric field. Correlated collisions in presence of high frequency electric field observed in numerical calculations of particle trajectories [1,8] remove this singularity and dominate heating rate for $v_0 < v_E$.

B. Numerical model

Our simulations of nonrelativistic electron scattering in the field of an ion with a charge Ze and in the presence of a uniform laser field are similar to the studies by Fraiman et al. [1]. However, in order to account for the physics which is outside the classical formulation of the test particle problem, we introduce an effective potential $U(x)$ [20]

$$U(r) = \frac{Ze^2}{r} \left[1 - \exp\left(-\frac{r}{B}\right) \exp\left(-\frac{r}{D}\right) \right]; \quad (5)$$

which has cut-offs both at large and small distances. It corresponds to the screened Coulomb potential at large distances and thus it accounts for plasma polarization effects. At short distances, it accounts for quantum diffraction effects at the de Broglie wavelength λ_B . Electron dynamics are described by the Newton's equation of motion

$$m \ddot{r} = -eE \sin(\omega t - kr) - \nabla U(r); \quad (6)$$

To show differences between the effective potential (5) and the bare Coulomb potential $U=1/r$, we present both functions in Fig. 1 together with characteristic distances which can limit the model (6) applicability. The de Broglie wavelength λ_B is calculated at the quiver velocity amplitude v_E corresponding to a laser intensity of 10^{16} W/cm^2 and a wavelength of $0.25 \text{ }\mu\text{m}$.

Numerical solutions of Eq. (6) require special attention regarding the choice of a suitable time step in the computation of electron orbits near the Coulomb scattering center. We have used the symplectic integration algorithm [21], which ensures good accuracy. Even though the test particle problem described by Eq. (6) appears simple, the construction of the statistical ensemble of results for a broad range of initial conditions for the averaging of heating rates poses considerable challenges in terms of computer memory and time requirements.

The IB heating rate for a single electron has been calculated directly from the simulation results according to the following equation:

$$\frac{d}{dt} = \frac{1}{2} n_i v_0 m \langle \dot{v}_0^2 - v_0^2 \rangle; \quad (7)$$

where v_0 and \dot{v}_0 are the electron drift velocities before and after a collision, angular brackets denote an averaging over the field phases and χ is the impact parameter. The drift velocity of an electron is defined as the difference between the total electron velocity and the quiver velocity (see Fig. 2 for details). The electron heating rate due to IB absorption (7) is compared below with known analytical and numerical results.

The dependence of the e-i scattering problem on the laser frequency ω , the electric field amplitude and the initial kinetic energy of an electron can be characterized in terms of two dimensionless parameters $\eta = \omega / (Ze^3/m^2)^{1/4}$ and v_0/v_E [1]. The ratio of the initial drift velocity to the quiver velocity amplitude, v_0/v_E , characterizes every IB theory, including quantum and classical analytical studies. The second parameter, η , defines the argument in the Coulomb logarithm in the classical limit, where the short distance cut-off involves the impact parameter for 90° scattering, $b_{max} = b_{min} = m v_0^3 / 2Ze^2 = (v_0/v_E)^3 \lambda_B = 2$; However, for the quantum cut-off, a new parameter appears which is $b_{max} = b_{min} = m v_0^2 / \hbar \omega = 2$.

Correlation effects which give rise to enhanced heating rates are due to the fast oscillation of electrons in the laser field. They bring an electron close to the ion many times as it crosses an interaction region. These effects are most pronounced at low drift velocities. For a drift velocity smaller than the quiver velocity, $v_0/v_E = v_0 < 1$, the electron trajectory becomes irregular [8] and it cannot be approximated by a straight path in the calculations of the collision cross-section.

III. IB HEATING RATES FOR DIFFERENT ELECTRON VELOCITY DISTRIBUTIONS

A. Electron beam-laser field energy exchange

Consider first a monoenergetic electron beam propagating in the direction of the laser electric field. This well defined geometry allows further simplifications of the IB heating rate expressions obtained with the KW cross section, Eq. (1),

$$\frac{d}{dt} = \frac{n_i Z^2 e^4}{m v_0} \int_{b_{min}}^{b_{max}} \frac{1}{b} \frac{1}{1 + \frac{p}{Z}} \frac{1}{1 + \frac{1}{b}} \frac{dy}{(y + \frac{1}{2})^2} J_1^2 \frac{2v_E y}{v_0}; \quad (8)$$

and in the IB heating rate obtained from the Dawson-Oberman theory, Eq. (2),

$$\frac{d}{dt} = \frac{4 n_i Z^2 e^4 X^2}{m v_0} \ln \left[\frac{2 J_1^2 (h v_E = v_0)}{1 + \frac{2 m^2 v_0^4}{h^2}} \right] \quad (9)$$

$$\frac{h v_E}{v_0} J_1 \quad \frac{h v_E}{v_0} \quad J_1 \quad \frac{h v_E}{v_0} \quad J_{l+1} \quad \frac{h v_E}{v_0} \quad \ln \left[1 + \frac{m^2 v_0^4}{h^2} \right] :$$

Equation (9) follows from Eq. (2) after integration over the transferred momentum k with the upper limit cut-off at $k_{max} = m v_0/h$, which corresponds to quantum short distance cut-off at the de Broglie length calculated at the initial electron drift velocity, $k_{min} = h/m v_0$. A more detailed study of the quantum mechanical expression (8) can be found in Ref. [22], where it is shown that an enhancement of the total cross-section occurs for $v_0 > v_E$ and an oscillatory behavior is observed for $v_0 < v_E$. Note, that in the classical limit, $l = 1$, Eq. (8) gives an expression which is similar to Eq. (9).

In the limit of a weak electric field, where $v_E = v_0$, $l = 1$; we recover from Eq. (8) the well known expression

$$\frac{d}{dt} = \frac{4 n_i Z^2 e^4 v_E^2}{m v_0^3} \ln \left[\frac{2 m v_0^2}{h} \right] \quad (10)$$

Figure 3 shows a comparison between the heating rates derived from the various theories described above, the classical approximation (3) and the numerical simulations. For large velocities $v_0 > v_E$ all approximations lead to similar results: $d = dt / v_0^3$. They can be calculated from the Rutherford scattering theory by accounting for the effect of a high frequency field in the Born approximation. Heating rates for $v_0 > v_E$ are negative, that is, the electron loses its energy due to emission of photons. This can be readily seen from the classical formula (3). For $v_0 < v_E$ the heating rates become positive and increases at first with decreasing electron drift velocity. Figure 3 clearly displays large discrepancies between the various approximations at $v_0 < v_E$. The $v_0 < v_E$ regime of velocities in the parallel launch geometry contains the so-called "representative" electrons of Ref. [1]. These are particles which undergo multiple scattering and follow complicated trajectories in the combined electric field of the scattering center and the high-frequency radiation. None of the analytical approaches can properly describe such interactions. The classical mechanical models rely on the assumptions of instantaneous collisions and small momentum exchange. Quantum results also fail to describe large angle scattering events. Two of the heating rates shown in Fig. 3 are obtained from numerical simulations: the black dots represent calculations for the bare Coulomb potential and follow the Fraiman et al. [1] results. The solid curve has been obtained by using the effective potential (5) with the de Broglie cut-off calculated at the initial electron drift velocity v_0 . These results involve an averaging with respect to phases of the oscillatory field.

The growth of the IB heating rate for small drift velocity electrons led Fraiman et al. [1] to suggest that the effective scattering cross section behaves as $\propto 1/v_0^2$. However, this unlimited growth is produced by slow electrons approaching ions at very close distances, which should be cut-off due to quantum effects. Elimination of such close encounters through the introduction of the effective Coulomb potential U (5) leads to much slower growth of the heating rate (solid line in Fig. 3).

The calculations based on the classical mechanical formulation require a short distance cut-off in order to, at least approximately, account for quantum effects. All analytical theories in Fig. 3 contain such a limitation, which results in the saturation of the heating rates at low drift velocities. The quantum KW theory (dot-dash curve) does not lead to a divergence. For small oscillatory fields KW theory produces a natural cut-off at $v_B(v_0)$ in the logarithmic term. However, its usefulness at low velocities in defining the proper quantum cut-off or the effective potential is limited as the theory fails to account for large momentum scattering events. The effects of electron capture and bound states are also absent from these calculations. For the parallel launch geometry of Fig. 3 an uncertainty in the choice of the quantum cut-off limits the validity of classical mechanical simulations, particularly because the results are very sensitive to the cut-off value.

Figure 4 examines another polarization of the initial electron velocity, which is now directed transversely to the direction of the oscillating field. In that case the heating rate is always positive. As in the case of a parallel launch, the heating rate increases for small electron drift velocities. However, it does not display any of the previous rapid changes or unique behavior in the vicinity of $v_0 = v_E$. Numerical simulations with the effective potential U (5) result in the reduction of the heating rate (solid line) as compared to the KW or the classical analytical model. We have also examined the electron phase space, finding no random trajectories or "representative" electrons undergoing large angle collisions.

B. IB heating rate for non-Maxwellian anisotropic electron velocity distribution function

Studies of monoenergetic electron scattering confirm the sensitivity of the heating rates to the relative orientation of the initial velocity and the electric field, as well as to details of the cut-off distance for short range interactions. The parallel launch geometry gives rise to random electron trajectories, multiple collisions and a large momentum exchange, all of which lead to an enhancement of the heating rate. The magnitude of this increase for typical conditions found in laser-produced plasmas depends on the number of slow electrons and the anisotropy of the actual electron distribution function. Plasmas produced by high intensity ultrashort laser pulses, if dominated by the multiphoton ionization [18] are characterized by anisotropic electron distribution functions. This can potentially lead to many large angle collisions resulting in an enhancement of the IB heating rates.

The velocity distribution function of photoelectrons is dependent on atomic and laser parameters. It displays a strong anisotropy along the direction of the linearly polarized laser beam [18,23]. The following simple analytical expression captures the main features of electrons produced by the multiphoton ionization process [23]:

$$F_0 = n_e (m/2 T_{eff})^{1/2} (v_x) \exp(-m v_x^2/2 T_{eff}) \quad (11)$$

where $T_{eff} = (3/2) m v_E^2 (J_h = J_{ion})^{3/2} E_0 / E_a$ is the effective temperature of photoelectrons, $E_a = e/a_B = 5.1 \text{ GV/cm}$ is the atomic electric field, a_B is the Bohr radius, J_{ion} is the ionization potential of the atom, and $J_h = e^2/2a_B$ is the first ionization potential of hydrogen.

We compare results of various analytical models and numerical simulations after averaging with respect to the electron distribution function (11). This averaging reduces to a simple integration of heating rate expressions in the parallel geometry (8) and (9) with a one-dimensional Maxwellian velocity distribution. The main contribution to this integral comes from slow electrons. In this region, all classical theories give different results that are strongly dependent on the cut-off parameters as has been shown above. For the quantum approach, the IB heating rate per electron as derived from Eq. (8) has the following form:

$$\frac{d}{dt} = n_i Z^2 e^4 \frac{r}{2T} \int_{l_E}^{\infty} \int_{-l_E}^{l_E} \int_{-l_E}^{l_E} du \exp\left(-\frac{m v_E^2}{2T} u^2\right) \int_{u-\frac{p}{u^2+E}}^{u+\frac{p}{u^2+E}} dy \frac{J_1^2(2y-E)}{(yu+E)^2}; \quad (12)$$

where $E = 2h/m v_E^2$.

Figure 5 represents the intensity dependence of the IB heating rates, that are obtained from our numerical model and from various analytical expressions we derived by using the single electron energy exchange rates averaged over an anisotropic distribution function (11). A relatively large discrepancy between various models follows from differences already shown in Fig. 3. An enhancement of the heating rate and a sensitivity to the cut-off values is characteristic for the parallel launch geometry. It is evident that the correlated collisions significantly enhance the heating rate at large intensities. The anisotropy of the electron distribution is responsible for such an effect. This fact is illustrated by comparison with the heating rate calculated for the three-dimensional Maxwellian (isotropic) distribution function

$$F_M = n_e (m/2 T_e)^{3/2} \exp(-m v^2/2 T_e) \quad (13)$$

with the same temperature, $T_e = T_{eff}$. In this case, the heating rate is reduced and displays a monotonic dependence on the laser intensity.

Photoionized plasmas with a non-Maxwellian distribution of electrons is another case where large angle collisions can lead to enhanced IB heating rates. More work needs to be done in comparing these models with experiments.

C. IB heating rate for an isotropic electron distribution

This section addresses the statistical significance of multiple collisions and random electron trajectories in the case of an isotropic electron distribution. Isotropic distribution functions are common in laser-produced plasmas as they are established after the ionization stage due to electron-electron and electron-ion collisions. By directly averaging the IB heating rate over all directions of initial velocities, we examine the relative importance of electrons which move parallel to the electric field vector. These have been identified in Ref. [1] and above, as the source of the enhancement in the IB heating rate. By taking an average with respect to a Maxwellian distribution function (13) with a temperature T_e , the quantum mechanical result (1) gives the following heating rate per electron

$$\frac{d}{dt} = \frac{r}{T_e} \frac{16n_i Z^2 e^4 v_E^2}{h!} \sum_{l=1}^{\infty} \frac{1}{l \sinh \frac{lh!}{2T_e}} \int_0^Z \frac{dq}{q^4} I_l(q) \exp \left[-\frac{l^2 m v_E^2}{2q^2 T_e} - \frac{q^2 h^2 l^2}{8m v_E^2 T_e} \right]; \quad (14)$$

The classical mechanical theory expression (2) gives

$$\frac{d}{dt} = \frac{p}{2m} \frac{8n_i Z^2 e^4 v_E^2}{T_e^{3/2}} \sum_{l=1}^{\infty} \frac{1}{l^2} \int_0^{q_m} \frac{dq}{q^4} I_l(q) \exp \left[-\frac{l^2 m v_E^2}{2q^2 T_e} \right]; \quad (15)$$

where $I_l(x) = \int_0^x J_1^2(y) dy$. The parameter $q_m = 2h! = T_e$ defines the cut-off at small distances. One can define an effective collision frequency: $d = dt = \frac{1}{\nu_{eff} m v_E^2} = 2$ and use Eqs. (14) and (15) to evaluate it. Figure 6 illustrates the variation of the effective collision frequency with $v_E = v_{Te}$ where $v_{Te} = (T_e/m)^{1/2}$ is the electron thermal velocity. Remarkably, all models and numerical simulations converge for large field values $v_E > v_{Te}$. No effects of correlated collisions can be observed. Discrepancies at small field values ($v_E < v_{Te}$) have more to do with differences between theoretical approximations, in particular, with the treatment of short range interactions. A simple approximation from Ref. [12,24] gives

$$\nu_{eff} = \nu_{ei} (1 + v_E^2 = 6v_{Te}^2)^{3/2}; \quad (16)$$

which provides a reasonable fit to results of all studies.

IV. CONCLUSIONS

We have performed numerical simulations based on the test particle model which involves classical electron trajectories in the combined electric field of an ion and a homogeneous, high frequency laser field. The representative results have been compared with existing analytical theories to test the numerical results and to illustrate the differences of our findings from current understanding of collisional processes in laser plasmas. We have confirmed the recent results by Fraiman et al. [1] and Wiesenfeld [8] regarding the existence of irregular electron orbits that closely approach an ion many times during each scattering event and lead to large angle deflections and large changes in the electron momentum. These "anomalous" collisions have been ignored in preceding theories which significantly underestimated the electron heating rates under certain conditions. The irregular electron trajectories may increase the IB heating rates in the regime of large-amplitude electric fields, $v_0 < v_E$, and for electron velocities parallel to the electric field of the laser. The magnitude of this enhancement depends on details of the potential at short distances and on the form of electron distribution anisotropy.

When the quantum short-distance cut-off is introduced through an effective potential, we have found a much smaller effect as compared to Fraiman et al. [1] who have used the bare Coulomb potential and have predicted an increase in the heating rate which is inversely proportional to the electron drift velocity. In addition, electrons which are responsible for this anomalous heating rate are statistically insignificant in the case of an isotropic electron distribution function. On the contrary, for highly anisotropic electron distributions such as that produced by photoionization, the new effect of large angle scattering dominates the heating rate at high laser intensities. This prediction could easily be compared with observations.

This work was partly supported by the Natural Sciences and Engineering Research Council of Canada and the Russian Foundation for Basic Research (grant N 00-02-16063).

-
- [1] G.M. Fraiman, V.A. Mironov, and A.A. Balakin, Phys. Rev. Lett. 82, 319 (1999); JETP 88, 254 (1999); G.M. Fraiman, A.A. Balakin, and V.A. Mironov, Phys. Plasmas 8, 2502 (2001).
 - [2] J. Dawson, C. O'Brien, Phys. Fluids 5, 517 (1962).
 - [3] V.P. Silin, Sov. Phys. JETP 20, 1510 (1965).
 - [4] F.B. Bunkin, A.E. Kazakov, and M.V. Fedorov, Sov. Phys. Uspekhi 15, 416 (1972); F.V. Bunkin and M.V. Fedorov, Sov. Phys. JETP 22, 844 (1966).
 - [5] N.M. Kroll and K.M. Watson, Phys. Rev A 8, 804 (1973).
 - [6] G.J. Pert, J. Phys. A: Gen. Phys. 5, 506 (1972).

- [7] P. M ulser, F. Comolti, F. Besuelle, and R. Schneider, *Phys. Rev. E* 63, 016406 (2001).
- [8] L. W iesenfeld, *Phys. Lett. A* 144, 467 (1990).
- [9] G. J. Pert, *J. Phys. B: Atom. Molec. Phys.* 12, 2755 (1979).
- [10] C. D. Decker, W. B. Mori, J. M. Dawson, and T. Katsouleas, *Phys. Plasmas* 1, 4043 (1994)
- [11] G. Shvets, N. J. Fish, *Phys. Plasmas* 4, 428 (1997).
- [12] D. Vick, C. E. Capjack, V. T. Tikhonchuk, and W. Rozmus, *Comments Plasma Phys. Cont. Fusion* 17, 87 (1996).
- [13] P. J. Catto and Th. Speziale, *Phys. Fluids* 20, 167 (1977).
- [14] S. Ichimaru, *Statistical plasma physics*, Addison-Wesley (Redwood City, 1992).
- [15] F. Ehlotzky, A. Jaron, and J. Z. Kaminski, *Phys. Reports*, 297, 63 (1998).
- [16] G. Ferrante, C. Leone, and L. LoCasio, *J. Phys. B* 12, 2319 (1979).
- [17] L. Schlessinger and J. Wright, *Phys Rev. A* 20, 1934 (1979).
- [18] P. B. Corkum, N. H. Burnett, and F. Brunel, *Phys. Rev. Lett.* 62, 1259 (1989); N. H. Burnett and P. B. Corkum, *J. Opt. Soc. Am. B* 6, 1195 (1989).
- [19] G. J. Pert, *Phys Rev. E* 51, 4778 (1995).
- [20] C. Deutsch, *Phys. Lett. A* 60, 317 (1977).
- [21] J. Candy, W. Rozmus, *J. Comp. Phys.* 92, 230 (1991).
- [22] R. Daniele, F. Trombetta, G. Ferrante, P. Cavaliere, and F. Morales, *Phys Rev. A* 36, 1156 (1987).
- [23] V. Yu. Bychenkov and V. T. Tikhonchuk, *Laser Physics* 2, 525 (1992).
- [24] R. J. Faehland N. F. Roderick, *Phys. Fluids* 21, 793 (1978).

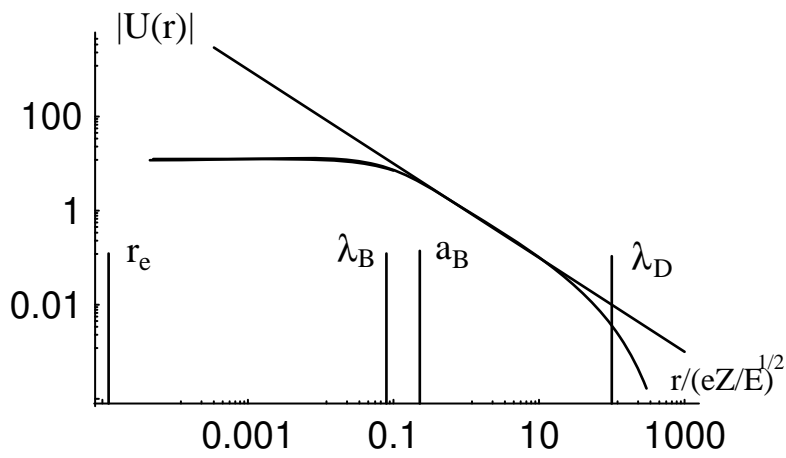


FIG. 1. Effective potential $|U(r)| = Z e^2 / (5r)$ in comparison with the bare Coulomb potential $1/r$. Characteristic dimensions are also shown - the Debye screening length, λ_D for an electron temperature 1 keV and density 10^{20} cm^{-3} ; the electron de Broglie length, λ_B for a laser intensity 10^{16} W/cm^2 and wavelength 0.25 μm ; the Bohr radius, a_B ; and the classical electron radius, r_e . Here $Z = 10$:

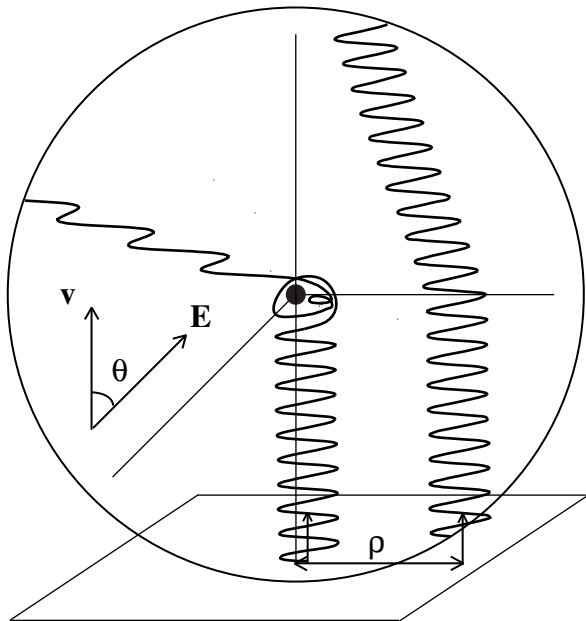


FIG. 2. Schematic electron orbits in the problem of e-i scattering in the laser field. Two typical electron trajectories are shown.

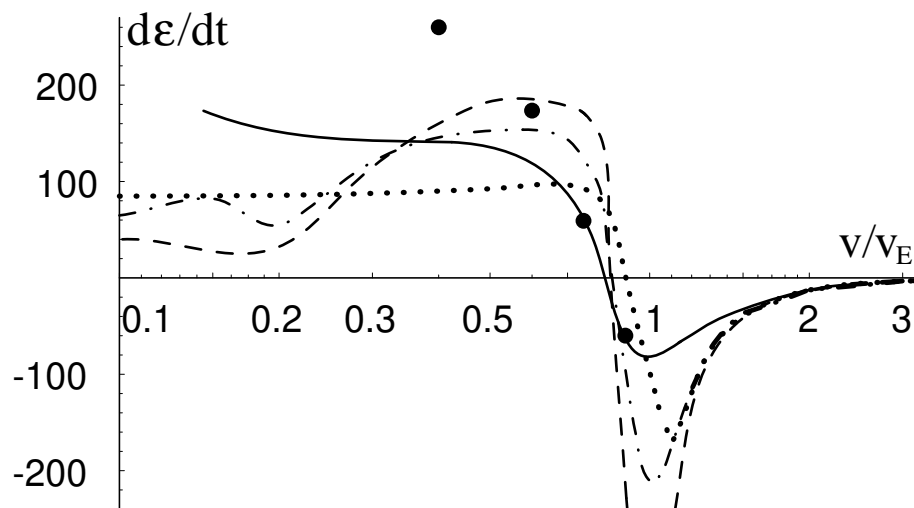


FIG. 3. Electron velocity dependence of the heating rate $d\epsilon/dt$ normalized to $n_i Z^2 e^4 / m v_E$ for the parallel launch geometry. The parameters are: $Z = 10$, the laser wavelength $0.25 \mu\text{m}$ and the intensity $4.43 \cdot 10^{16} \text{ W/cm}^2$. Solid curve demonstrates the numerical results, the KW approximation - dash-dotted line, the Dawson-Oberman approach - dashed line, the classical approach - dotted line. The black dots represent the numerical simulations with the bare Coulomb potential.

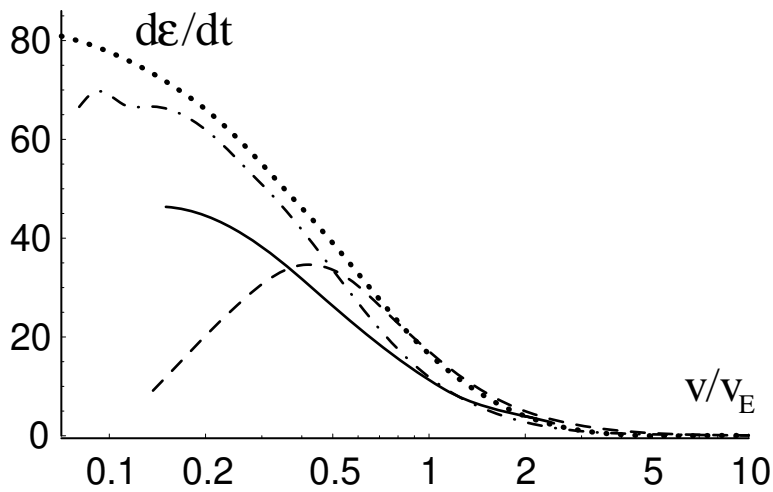


FIG. 4. Electron velocity dependence of the heating rate $d\epsilon/dt$ for the perpendicular launch geometry and for the same laser and plasma parameters as in Fig. 3: the numerical results - solid curve, the KW approximation - dash-dotted line, the Dawson-Oberman approach - dashed line, the classical approach - dotted line.

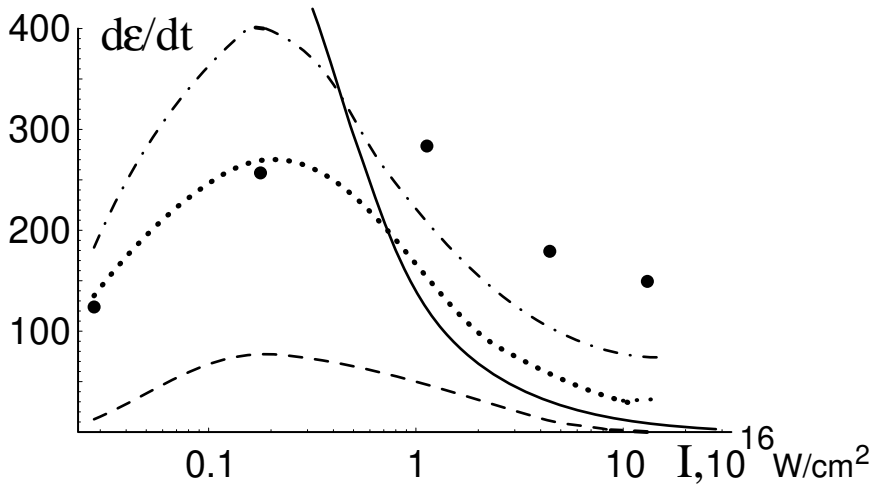


FIG. 5. Laser intensity dependence of the absorption rate per electron $d\epsilon/dt$ normalized to $\frac{P}{2} \frac{1}{n_i Z^2 e^4} \frac{1}{m c}$ for the laser wavelength $0.25 \mu\text{m}$, averaged on an anisotropic distribution function (11): numerical results - points, the KW approximation - dash-dotted line, the Dawson-Oberman approach - dashed line, the classical approach - dotted line. Here $J_{ion} = J_h = 1$: Solid line gives the heating rate with isotropic Maxwellian distribution of the same temperature.

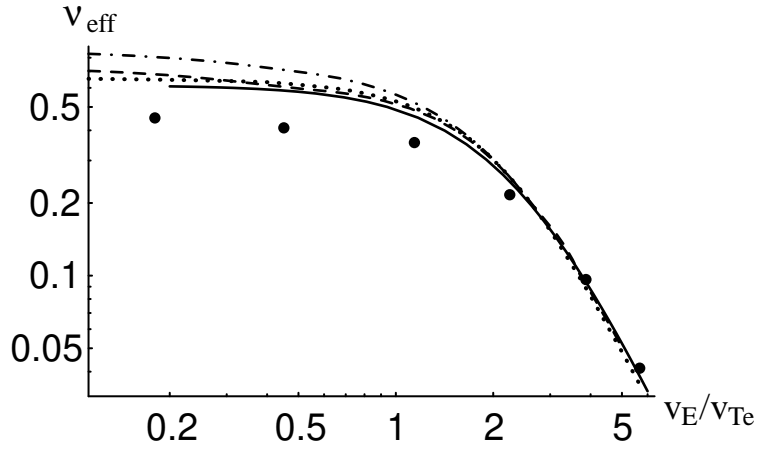


FIG. 6. Dependence of the effective absorption frequency ν_{eff} ; normalized to $16 \frac{P}{2} \frac{1}{n_i Z^2 e^4} \frac{1}{m^2 v_{Te}^3}$; on $\nu_E = \nu_{Te}$ for a plasma with $Z = 10$, $T_e = 200 \text{ eV}$ and for the Maxwellian electron distribution function: numerical results - points, the KW approximation - dash-dotted line, the Dawson-Oberman approach - dashed line, the classical approach - dotted line. Solid line gives approximation (16). Here, the laser wavelength is $0.25 \mu\text{m}$.